Acta Crystallographica Section F
Structural Biology and Crystallization Communications
ISSN 1744-3091

Sequence-induced trimerization of phospholipase A_2: structure of a trimeric isoform of PLA_2 from common krait (*Bungarus caeruleus*) at 2.5 Å resolution

Garima Singh,[a] S. Gourinath,[a] K. Saravanan,[a] Sujata Sharma,[a] S. Bhanumathi,[b] Ch. Betzel,[b] A. Srinivasan[a] and T. P. Singh[a]*

[a]Department of Biophysics, All India Institute of Medical Sciences, New Delhi, India, and [b]Institute of Medical Biochemistry and Molecular Biology, Hamburg, Germany

Correspondence e-mail: tps@aiims.aiims.ac.in

Received 30 September 2004
Accepted 11 October 2004
Online 16 October 2004

PDB Reference: krait trimer PLA_2, 1g2x, r1g2xsf.

The venom of the common Indian krait (*Bungarus caeruleus*) contains about a dozen isoforms of phospholipase A_2 (PLA_2), which exist in different oligomeric forms as well as in complexes with low-molecular-weight ligands. The basic objective of multimerization and complexation is either to inactivate PLA_2 in the venom for long-term storage, to generate a new PLA_2 function or to make a more lethal assembly. The current isoform was isolated from the venom of *B. caeruleus*. Dynamic light-scattering studies indicated the presence of a stable trimeric association of this PLA_2. Its primary sequence was determined by cDNA cloning. The purified protein was crystallized with 2.8 *M* NaCl as a precipitating agent using the sitting-drop vapour-diffusion method. The crystals belonged to the monoclinic space group *C*2, with unit-cell parameters a = 80.9, b = 80.5, c = 57.1 Å, β = 90.3°. The structure was refined to a final *R* factor of 0.198. This is a novel trimeric PLA_2 structure in which the central pore formed by the association of three molecules is filled with water molecules. The interactions across the pore take place *via* multiple water bridges primarily to the side chains of Arg, Lys and Thr residues. Approximately 12% of the total solvent-accessible surface area is buried in the core of the trimer. The active sites of all three molecules are located on the surface and are fully exposed to the solvent, resulting in a highly potent enzymatic unit.

1. Introduction

Phospholipase A_2 (PLA_2; EC 3.1.1.4) catalyzes the hydrolytic cleavage of 1,2-di-acyl-3-*sn*-phosphoglycerides, releasing fatty acids and lysophospholipids (van Deenen & de Haas, 1963). These enzymes are widely distributed in the animal world. Recently, PLA_2s have also been reported from plants (Stahl *et al.*, 1998, 1999; Kim *et al.*, 1999) and from prokaryotic sources (Sugiyama *et al.*, 2002). In addition to the basic catalytic function, these proteins are also found to possess many pharmacological properties such as neurotoxicity, cardiotoxicity, myotoxicity, platelet aggregation, anticoagulant effects *etc.* (Kini & Evans, 1989). These cysteine-rich proteins (ten, 12 or 14 cysteines per sequence) contain between 119 and 134 amino-acid residues. PLA_2s from different sources share common qualitative catalytic properties but differ greatly in their pharmacological properties. Following broad classification into extracellular and intracellular types, the secretory enzymes have been further divided into many groups and subgroups mainly based on sequence criteria (Scott & Sigler, 1994). The most extensively studied of these are the group I and group II enzymes, which are highly homologous and share similar kinetic behaviour (Heinrikson, 1991). Group I contains enzymes from mammalian pancreatic species and from Elapidae (cobras) and Hydrophiidae (sea snakes) snake venoms, mammalian exocrine pancreas and human spermatozoa (Langlais *et al.*, 1992), whereas PLA_2s from Crotalidae (rattlesnakes and pit vipers), Viperidae (old world vipers), human synovial fluid, a variety of mammalian cell types including platelets, gastric mucosa, neutrophils and vascular endothelium (Kramer *et al.*, 1989; Komada *et al.*, 1989; Kurihara *et al.*, 1991; Rosenthal *et al.*, 1995) belong to group II. Members of the first group possess an S—S bridge between the side chains of Cys11 and Cys80. The enzymes of the second group have a C-terminal extension of five to seven residues including a C-terminal Cys residue linked to the SH group of residue 50. The other six disulfide bridges are conserved in proteins from both groups.

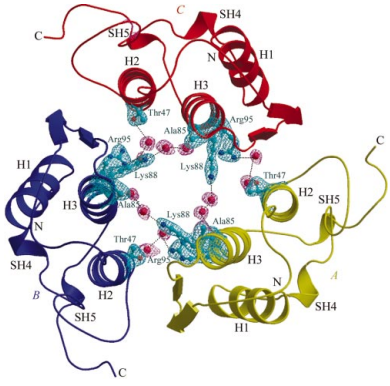

The current PLA_2 from *Bungarus caeruleus* belongs to group I. Of all known PLA_2 structures, only two other trimeric structures, those of PLA_2s from *Naja naja naja* (Fremont *et al.*, 1993; Segelke *et al.*, 1998) and *N. naja kaouthia* (Gu *et al.*, 2002), have been determined so far. Here, we report the crystal structure of a novel trimer of PLA_2 from *B. caeruleus* at 2.5 Å resolution.

2. Experimental procedures

2.1. Purification of PLA_2

Lyophilized *B. caeruleus* venom was obtained from Irula co-operative snake farm, Tamil Nadu, India and purified as reported previously (Singh *et al.*, 2001). 1 g of venom was dissolved in de-ionized water to a concentration of 50 mg ml^{-1}. This was centrifuged at 8000*g* for 15 min to remove insoluble material. The supernatant was applied to a CM-Sephadex C-25 cation-exchanger (60 × 1 cm) that had been equilibrated with 0.05 *M* ammonium acetate pH 5.0 at 277 K. Proteins adsorbed on the column were eluted with a linear gradient of ammonium acetate from 0.05 *M* at pH 5.0 to 0.5 *M* at pH 7.0. The purified PLA_2 samples were pooled and lyophilized.

2.2. Dynamic light scattering

The sample solutions for the experiment were prepared in 50 m*M* Tris–HCl buffer pH 8.0 made with deionized water from a Millipore Alpha-Q system. The samples were filtered through 0.1 µm polyvinylidene difluoride filters (Millipore). The enzyme concentration varied from 5.0 to 15.0 mg ml^{-1}. Samples were manually injected into a flow cell (30 µl) and illuminated by a 30 mW, 660 nm laser diode. The dynamic light-scattering (DLS) data were collected in quintuplicate using a Spectroscatter 201 (RiNA Netzwerk RNA-Technologien, Berlin, Germany) laser at a temperature of 303 K and the results were analyzed with *Xmgr* v. 3.01 software (Turner, 1991).

2.3. Sequence determination

B. caeruleus venom glands were obtained from Irula Snake Catchers Cooperative Society, Chennai with the permission of the Government of Tamil Nadu. The minced glands were stored in 4 *M* guanidine isothiocyanate solution at 203 K prior to use. The tissues were homogenized in a Polytron (Kinematica, Switzerland) homogenizer. The total RNA was extracted with an equal volume of a 1:1 phenol–chloroform mixture. Quantification of RNA was performed spectrophotometrically. 10 µg total RNA was used for cDNA synthesis using Revert Aid M-MuLV reverse transcriptase (MBI, Lithuania) and oligo-$(dT)_{18}$ primer MBI. The conserved nucleotide sequences of group I PLA_2s were used for construction of primers. The oligonucleotides 5′ AAA TGT ATC CTG CTC ACC TTC T 3′ and 5′ GCT GAA GCC TCT CAA ATA TCA T 3′ were used as forward and reverse primers in PCR amplification using a PTC 100 thermocycler (MJ Research, USA). The amplified product of 464 bp was cloned in a pGEMT (Promega, USA) vector. Automated DNA sequencing of the insert was performed with an ABI-377 sequencer (ABI Biosystems, USA). Both strands were sequenced. The cDNA reported here comprises an ORF encoding 147 amino acids and a 3′ UTR of 18 bp. The sequence was submitted to GenBank (accession No. AY455756).

2.4. Crystallization of PLA_2

Crystals of PLA_2 were obtained using the sitting-drop vapour-diffusion method. The protein sample was dissolved at 5 mg ml^{-1} in 50 m*M* Tris–HCl buffer pH 8.5 containing 1.4 *M* NaCl, 1 m*M* NaN_3. It was equilibrated against the same buffer containing 2.8 *M* NaCl. After 3 d incubation at 281 K, crystals had grown to about 0.3 × 0.2 × 0.2 mm in size.

Table 1
Crystallographic data and refinement statistics.

Values in parentheses are for the last resolution shell.

PDB code	1g2x
Space group	*C*2
Unit-cell parameters	
a (Å)	80.9
b (Å)	80.5
c (Å)	57.1
β (°)	90.3
Resolution range (Å)	20.0–2.5 (2.6–2.5)
No. unique reflections	12745
Completeness (%)	99.9 (99.6)
R_{sym} (%)	9.1 (20.3)
$I/\sigma(I)$	7.8 (2.3)
R factor/R_{free} (%)	19.8/26.2
R.m.s. deviations in *B* factors	
Main-chain atoms (Å^2)	0.8
Side-chain atoms (Å^2)	1.3
R.m.s. deviations in bond lengths† (Å)	0.007
R.m.s. deviations in bond angles† (°)	1.3
Overall average *G* factor‡	0.55

† Target stereochemistry from Engh & Huber (1991). ‡ *G* factor as reported by *PROCHECK* (Laskowski *et al.*, 1993).

2.5. X-ray intensity data collection

The crystals diffracted to 2.5 Å resolution. The data were collected on EMBL beamline X-11 at DESY, Hamburg with λ = 0.98 Å using a MAR 345 imaging-plate scanner with 1.0° rotation for each image. A single crystal was mounted in a nylon loop and flash-cooled in a nitrogen stream at 100 K using 15% glycerol in reservoir buffer. The data were processed with *DENZO* and *SCALEPACK* (Otwinowski & Minor, 1997). The results of data collection and processing are given in Table 1.

2.6. Structure determination

The structure was solved by molecular replacement with the *AMoRe* program (Navaza, 1994) from the *CCP*4 software suite (Collaborative Computational Project, Number 4, 1994; Dodson *et al.*, 1997) and with the structure of the monomeric isoform of krait PLA_2 as a model (PDB code 1fe5; Singh *et al.*, 2001). The rotation function was calculated with diffraction data from 10 to 4.5 Å resolution within a sphere radius of 14 Å. The first three peaks in the output appeared as distinct solutions in the rotation function. These peaks grew more distinct in the translation calculations, with an overall correlation coefficient of 34.3% and an *R* factor of 49.9%. Rigid-body refinement further improved the correlation coefficient to 42.0% with an *R* factor of 46.2%.

2.7. Structure refinement

The solution was applied to model coordinates with *LSQKAB* (Collaborative Computational Project, Number 4, 1994) and they were used as the starting model for refinement in the *CNS* package (Brünger *et al.*, 1998). The reflections were treated as two data sets, one data set consisting of 5% of the reflections (637 reflections) which were randomly selected for free *R* calculations (Brünger, 1992) and the other set consisting of the remaining data (12 108 reflections). During refinement, the bond lengths and bond angles were restrained to be close to standard values; restraints were also placed on the planarity of groups and non-bonded contacts as defined by Engh & Huber (1991). Several cycles of refinement by rigid-body conjugate-

gradient minimization, simulated-annealing and model building with the program *O* (Jones *et al.*, 1991) lowered the *R* factor to 0.30 and R_{free} to 0.415 for all data in the resolution range 20.0–2.5 Å. At this stage, individual isotropic *B*-factor refinement was carried out, which reduced the *R* factor to 0.260 and R_{free} to 0.334. Manual model building into $|2F_o - F_c|$ and $|F_o - F_c|$ electron-density maps and further refinement by simulated annealing following a slow-cooling protocol from 3000 to 300 K (Brünger *et al.*, 1990) lowered the *R* factor to 0.234 and R_{free} to 0.321 for reflections in the resolution range 20.0–2.5 Å. Water molecules were included in the model provided that the peaks were greater than 2.5σ in $|F_o - F_c|$ maps and that the waters had hydrogen-bonding partners with appropriate distance and angle geometry and had *B* values less than 50 Å^2 after refinement. The refinement improved the map and enabled the addition of further water molecules. After each set of refinement cycles, $|2F_o - F_c|$ and $|F_o - F_c|$ maps were calculated using *MAPMAN* (Kleywegt & Jones, 1996) and corrections to the side-chain orientations were made in *O* (Jones *et al.*, 1991) on a Silicon Graphics Indigo-2 workstation. The model was checked by calculating a series of omit maps at each stage of refinement. An omit map calculated without channel water molecules or the side chains of residues Thr47, Ala85, Lys88 and Arg95, which are oriented towards the core of the trimeric channel, is shown in Fig. 1.

3. Results and discussion

3.1. Sequence of PLA_2

In order to distinguish it from other PLA_2 trimers, the present PLA_2 trimer will be referred to as the krait trimer in all subsequent comparisons. The cDNA reported here consists of an ORF of 441 nucleotides coding for 147 amino acids and a 3′ UTR of 18 bp including the stop codon (Fig. 2). The krait trimer isoform of PLA_2 shows a high sequence identity, ranging from 74 to 85%, with previously reported PLA_2s from the same venom (GenBank accession codes AY455754, AF297663 and AY455755). The sequence identity with other group I PLA_2s varies from 50 to 83%, but the sequence identity with group II PLA_2s is comparatively low, with values ranging from 29 to 56% (Kini, 1997). The only other trimer of PLA_2 with known coordinates and primary sequence is the cobra trimer (Fremont *et al.*, 1993). It is of great interest to examine the sequence differences between two trimers. The most critical differences between the sequences of krait trimeric PLA_2 and cobra trimeric PLA_2 that might have a bearing in their association correspond to the residues at positions 24, 46, 47, 75, 80, 81, 82 and 88. The amino acids in these positions have interactions that differ between the two structures.

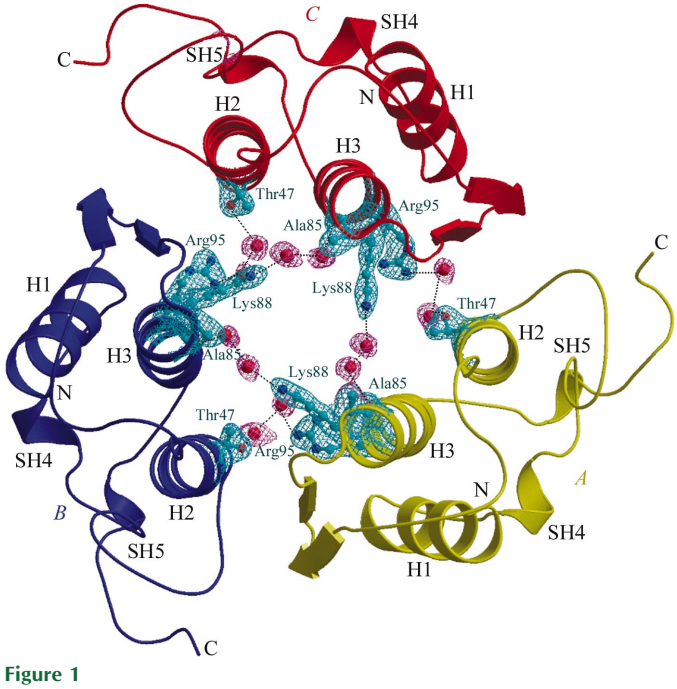

Figure 1
The overall fold of the trimer, showing monomers *A* (yellow), *B* (blue) and *C* (red). The secondary-structure elements are also indicated. The difference ($|F_o - F_c|$) Fourier map drawn at 2.5σ cutoff was calculated by omitting the contents of the trimeric pore. The figure was produced with the help of the programs *BOBSCRIPT* (Esnouf, 1997) and *RASTER3D* (Merritt & Murphy, 1994).

3.2. PLA_2 trimer

The DLS experiments carried out in the protein concentration range 5.0–15.0 mg ml^{-1} showed a mean hydrodynamic radius (R_H) of 2.99 nm for krait PLA_2, which corresponds to a molecular weight of approximately 42 kDa (Turner, 1991). This indicates the presence of a trimer in the solution state. Since the polydispersity value in these estimations is below 15% of the average radius, all PLA_2 molecules in solution exist in the trimeric form.

3.3. Overall structure

The final model consists of 2694 protein atoms from three molecules of krait PLA_2 designated *A*, *B* and *C*, and 261 water O atoms. The accuracy of the model of PLA_2 was checked during refinement by calculations of electron-density maps with $|F_o - F_c|$ coefficients and with selected parts of the molecule deleted from the atomic model used for structure-factor calculations. The final $|2F_o - F_c|$ electron-density map represents continuous and well defined density for the backbone as well for the side chains. The overall *B* factor for the structure was 29.2 Å^2. Refinement was completed satisfactorily and the final model is of good stereochemical quality (Table 1). A Ramachandran plot of the main-chain torsion angles (φ, ψ) (Ramachandran & Sasisekharan, 1968) calculated using *PROCHECK* (Laskowski *et al.*, 1993) showed that 89.4% of the residues were found in the most allowed regions and that the remaining residues

```
  1  ctg gta gcg gtt tgt gtc tcc ctc tta gga gcc gcc aac att     42
-19   Leu Val Ala Val Cys Val Ser Leu Leu Gly Ala Ala Asn Ile    -6
                          ▼
 43  cct ccc cag cct ctc aac ctg caa caa ttc aag aac atg att     84
 -5  Pro Pro Gln Pro Leu Asn Leu Gln Gln Phe Lys Asn Met Ile     9

 85  caa tgt gcc ggc act aga acc tgg aca gca tac atc aac tac     126
 10  Gln Cys Ala Gly Thr Arg Thr Trp Thr Ala Tyr Ile Asn Tyr     23

127  Ggt tgc tac tgc ggc aaa gga ggt agt ggg aca ccg gta gat     168
 24  Gly Cys Tyr Cys Gly Lys Gly Gly Ser Gly Thr Pro Val Asp     37

169  aag ttg gat agg tgc tgc tat act cat gac cac tgc tat aat     210
 50  Lys Leu Asp Arg Cys Cys Tyr Thr His Asp His Cys Tyr Asn     51

211  caa gct gac tca att cct gga tgc aac ccc aac ata aaa aca     252
 52  Gln Ala Asp Ser Ile Pro Gly Cys Asn Pro Asn Ile Lys Thr     65

253  tat tcc tat aca tgt act caa cct aat atc acc tgc act cgt     294
 66  Tyr Ser Tyr Thr Cys Thr Gln Pro Asn Ile Thr Cys Thr Arg     79

295  acg gca gac gct tgt gca aaa ttt ctt tgt gat tgt gac cgc     336
 80  Thr Ala Asp Ala Cys Ala Lys Phe Leu Cys Asp Cys Asp Arg     93

337  acg gca gcc atc tgc ttc gcg agt gca cca tac aac atc aac     378
 94  Thr Ala Ala Ile Cys Phe Ala Ser Ala Pro Tyr Asn Ile Asn     107

379  aat att atg att agc gca tct aat tct tgc caa tga             414
108  Asn Ile Met Ile Ser Ala Ser Asn Ser Cys Gln ***             118
```

Figure 2
Nucleotide and deduced amino-acid sequences of krait PLA_2. The arrow indicates the amino-terminus of the mature protein. The stop codon is indicated by ***. The cDNA sequence was deposited in GenBank with accession code AY455756.

were located in additionally allowed regions, with none in the generously allowed or disallowed regions.

The molecular topology of PLA_2 conserves all the main features of the PLA_2 folding. The N-terminal helix (H1) runs from residue 2 to residue 12. Helix 2 (H2) extends from residue 40 to residue 55, while helix 3 (H3) spans residues 85–103. The structure also contains a double-stranded antiparallel β-sheet designated the β-wing (residues 70–73 and 76–79). There are two helical turns involving residues 19–22 (SH4) and 108–110 (SH5) (Fig. 1). The backbone conformations of molecules *A*, *B* and *C* are essentially identical; the displacement of the C^{α} trace between the pairs of monomers is less than 0.4 Å. Least-squares superpositions of the C^{α} atoms of the present structure on equivalent C^{α} atoms of group I and group II PLA_2s (Kini, 1997) show r.m.s. shifts of 0.44–1.15 and 0.64–1.33 Å, respectively.

3.4. Trimeric association

Molecules *A*, *B* and *C* of krait PLA_2 form a symmetrical trimer (Fig. 1). The rotations between molecules *A* and *B*, *B* and *C*, and *C* and *A* are of the order of 120°, indicating the presence of a threefold non-crystallographic rotation axis. The molecules aggregate in such a way that the active sites of all three are accessible from the surface through hydrophobic channels with unhindered openings (Fig. 3*a*). The antiparallel helices H2 and H3 from the three monomers form the inner walls of an internal solvent channel in the trimeric structure (Fig. 1). The interior of this solvent channel is filled with water molecules. A number of well ordered water molecules are present in this trimeric pore and are involved in multiple hydrogen bonds with protein residues. The most prominent amino-acid residues that participate in these interactions are Thr47, Ala85, Lys88 and Arg95 (Fig. 1), showing that the core of the trimeric channel is primarily occupied by basic amino acids. The overall length of the solvent pore in this trimer is approximately 28 Å long, with a width varying between 13 and 17 Å. The buried area in the interface is of the order of 12% (Collaborative Computational Project, Number 4, 1994) of the total surface area of the trimer. There are at least 26 interactions between the adjacent molecules of the trimer. These involve direct links between protein atoms, consisting of 14 side chain–main chain interactions and 12 side chain–side chain interactions (Table 2). It is noteworthy that only a few solvent molecules are observed between the subunits.

Table 2
Intersubunit interactions in the trimer.

A/*B*/*C*	*B*/*C*/*A*	Distances (Å)
Gln74 O	Thr36 $O^{\gamma1}$	3.0
Thr73 $O^{\gamma1}$	Tyr46 OH	2.9
Thr78 $O^{\gamma1}$	Tyr46 OH	3.0
Cys79 O	Gln54 $N^{\varepsilon2}$	3.2
Thr82 $O^{\gamma1}$	Gln54 O	3.0
Thr80 O	OW18	3.0
OW18	Asn53 $N^{\delta2}$	3.1
Asn76 $N^{\delta2}$	OW194	2.7
OW194	Arg43 NH1	3.1
Lys88 N^{ζ}	OW28	3.1
OW28	OW24	2.5
OW24	Ala85 O	3.0

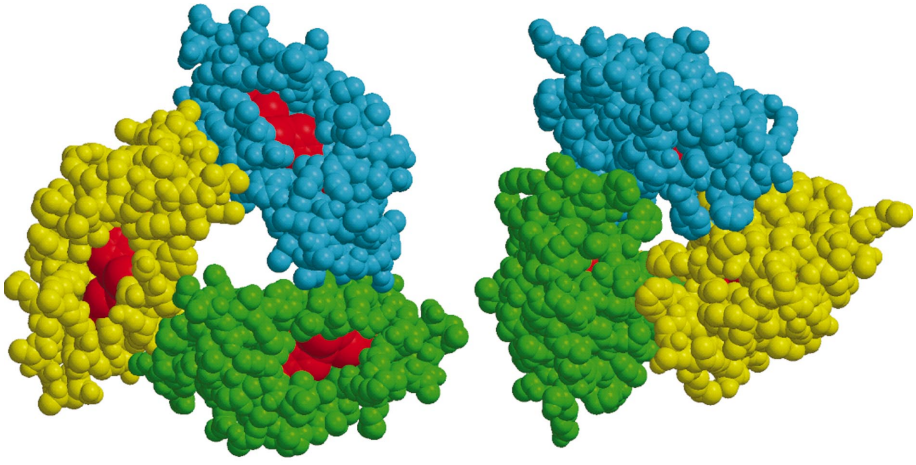

(*a*) (*b*)

Figure 3
(*a*) Monomers *A*, *B* and *C* (shown in cpk) in the krait trimer forming a highly potent active unit with active sites (red colour) fully exposed. (*b*) Monomers *A*, *B* and *C* (shown in cpk) in the cobra trimer showing the active sites (red colour) to be fully occluded. The figures were produced with *MOLSCRIPT* (Kraulis, 1991) and *RASTER3D* (Merritt & Murphy, 1994)

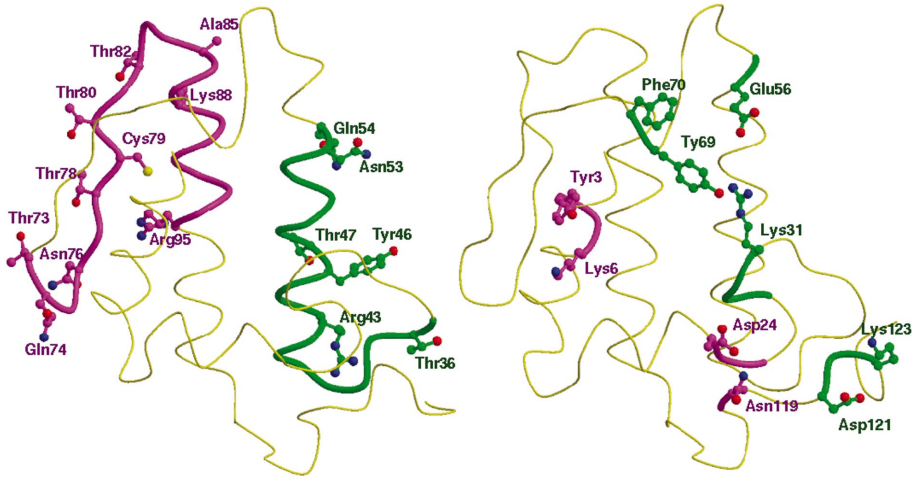

(*a*) (*b*)

Figure 4
The (*a*) krait and (*b*) cobra monomers showing the interfaces and residues (in green and magenta colours) involved in monomer–monomer interactions in the respective trimers.

3.5. Comparisons with other homotrimers

So far, five crystal structures of PLA_2 homotrimers have been reported. These include three essentially identical structures from *N. naja naja* (Fremont *et al.*, 1993; Segelke *et al.*, 1998), of which one contains Ca^{2+} and the other two do not. In the following, the structure containing Ca^{2+} will be used for comparison and will be referred to as cobra trimer. The two other structures (the same protein in two different space groups) are from *N. naja kaouthia* (a different subspecies; Gu *et al.*, 2002; PDB files for these structures are not available). The trimeric structure from *N. naja kaouthia* will be referred to as kaouthia trimer. The overall trimeric association as well as the

intersubunit contacts are strikingly different in these structures, although the dimensions of the cavity are similar in the three cases. The interior of the krait trimer is filled with solvent molecules linking Thr47, Ala85, Lys88 and Arg95 *via* water bridges across the trimeric pore. In contrast, the trimeric channel in cobra PLA_2 is predominantly occupied by hydrophobic residues such as Tyr3, Trp20 and Trp67 and solvent molecules are completely absent. Similarly, the trimeric cavity in kaothia PLA_2 is also filled with hydrophobic residues such as Leu2, Tyr3, Trp18, Trp19, Ala22, Leu63 and Phe64. Another striking difference corresponds to the location of the active sites. In the krait structure the hydrophobic channel opens to the outward surface of the monomeric units, while in the cobra trimer the active sites and hydrophobic channels are situated near the centre of the pore (Fig. 3*b*). Similarly, the entrances to the hydrophobic channels in kaouthia PLA_2 open into the trimer cavity. Furthermore, the contacts between adjacent monomers in the krait trimer are predominantly through hydrogen bonds involving residues Thr36, Tyr46, Glu54, Thr73, Glu74, Thr78, Cys79 and Thr82 (Fig. 4*a*). The interactions between adjacent monomers in the cobra trimer are primarily electrostatic and the residues involved are Tyr3, Lys6, Asp24, Arg31, Glu56, Asn119, Asp121 and Lys123 (Fig. 4*b*). In the kaouthia trimer, the intersubunit interactions include both hydrophobic and electrostatic interactions.

3.6. Catalytic activity of PLA_2

In krait PLA_2, the three catalytic residues His48, Tyr52 and Asp99 together with Asp49 display a stereochemistry that conforms ideally to that of the so-called 'catalytic network', a system of hydrogen bonds involving the catalytic residues (Verheij *et al.*, 1980). The side chains of His48, Tyr52 and Asp99 are directly bonded to each other, while that of Asp49 interacts with His48 through a water molecule. This unique water molecule is required for catalytic activity. The side chains of the active-site residues do not show appreciable deviations when superimposed on the active-site residues of the monomeric isoform of krait PLA_2 (Singh *et al.*, 2001). The active sites of all the monomeric units in the krait trimer are fully accessible from the surface, thus suggesting little change in the catalytic activities of the individual subunits. Therefore, the krait trimer as a unit presents three equivalent catalytic sites, making it a highly efficient arrangement. This is in striking contrast to both cobra and kaouthia trimers, whose active sites are found to be largely hindered in the trimeric arrangements.

3.7. Ca^{2+}-binding loop

In the calcium-binding loop of the krait trimer, one water molecule is present in each monomer. The conformations of the calcium-binding loops in the all three subunits are identical, with an r.m.s. shift of 0.4 Å for the C^{α} positions. C^{α} superposition of the calcium-binding loop of monomer *A* of the krait trimer with monomer *A* of the cobra trimer (PDB code 1a3f) gives an r.m.s. shift of 1.3 Å. Large shifts of 1.9, 2.7 and 2.3 Å are observed for residues 31, 32 and 33, respectively. Lys31 is involved in the formation of a salt bridge with residue 24, which is an aspartate in the case of cobra PLA_2 trimer and an asparagine in krait PLA_2.

3.8. Conclusions

Although PLA_2 has been observed to exist in a number of oligomeric forms, little is known about the significance of these oligomeric states with respect to its function. It has been shown that PLA_2 undergoes a concentration-dependent aggregation to dimeric or higher order states (Roberts *et al.*, 1977; Deems & Dennis, 1999). It has also been observed that oligomerization also occurs owing to the presence of specific amino acids at certain sites in the PLA_2 sequence. The consequences of oligomerization are expected to be observable in terms of the stability of the structure and modulation of its function. The manner in which subunits are aligned in krait PLA_2 trimer makes it a highly potent unit with three active sites on a highly ordered framework. In contrast, the cobra trimeric form is an inactive form of the enzyme with a considerably enhanced stability (Fremont *et al.*, 1993) and the trimer of kaouthia PLA_2 (Gu *et al.*, 2002) is a partially active state. These novel oligomeric states either promote or inhibit the catalytic activities of PLA_2, but all of them represent more stable forms than their monomeric structures.

The authors acknowledge financial support from Department of Science and Technology (DST), New Delhi under the FIST program. GS thanks the Council of Scientific and Industrial Research (CSIR), New Delhi for the award of a fellowship.

References

Brünger, A. T. (1992). *Nature (London)*, **355**, 472–474.
Brünger, A. T., Adams, P. D., Clore, G. M., DeLano, W. L., Gros, P., Grosse-Kunstleve, R. W., Jiang, J.-S., Kuszewski, J., Nilges, N., Pannu, N. S., Read, R. J., Rice, L. M., Simonson, T. & Warren, G. L. (1998). *Acta Cryst.* D**54**, 905–921.
Brünger, A. T., Krukowski, A. & Erickson, J. (1990). *Acta Cryst.* A**46**, 585–593.
Collaborative Computational Project, Number 4 (1994). *Acta Cryst.* D**50**, 760–763.
Deems, R. A. & Dennis, E. A. (1999). *Arch. Biochem. Biophys.* **366**, 177–182.
Deenen, L. L. M. van & de Haas, G. H. (1963). *Biochem. Biophys. Acta*, **70**, 538–553.
Dodson, E. J., Winn, M. & Ralph, A. (1997). *Methods Enzymol.* **277**, 620–633.
Engh, R. A. & Huber, R. (1991). *Acta Cryst.* A**47**, 392–400.
Esnouf, R. M. (1997). *J. Mol. Graph.* **15**, 132–134.
Fremont, D. H., Anderson, D. H., Wilson, I. A., Dennis, E. A. & Xuong, N.-H. (1993). *Proc. Natl Acad. Sci. USA*, **90**, 342–346.
Gu, L., Wang, Z., Song, S., Shu, Y. & Lin, Z. (2002). *Toxicon*, **40**, 917–922.
Heinrikson, R. L. (1991). *Methods Enzymol.* **197**, 201–214.
Jones, T. A., Zou, J., Cowan, S. W. & Kjeldgaard, M. (1991). *Acta Cryst.* A**47**, 110–119.
Kim, J. Y., Chung, Y. S., Ok, S. H., Lee, S. G., Chung, W. I., Kim, I. Y. & Shin, J. S. (1999). *Biochim. Biophys. Acta*, **1489**, 389–392.
Kini, R. M. (1997). *Venom Phospholipase A_2 Enzymes: Structure, Function and Mechanism*, pp. 146–147. Chichester: John Wiley & Sons.
Kini, R. M. & Evans, H. J. (1989). *Toxicon*, **27**, 613–635.
Kleywegt, G. J. & Jones, T. A. (1996). *Acta Cryst.* D**52**, 826–828.
Komada, M., Kudo, I., Mizushima, H., Kitamura, N. & Inoue, K. (1989). *J. Biochem. (Tokyo)*, **106**, 545–547.
Kramer, R. M., Hession, C., Johansen, B., Hayes, G., McGray, P., Chow, E. P., Tizard, R. & Pepinsky, R. B. (1989). *J. Biol. Chem.* **264**, 5768–577.
Kraulis, P. J. (1991). *J. Appl. Cryst.* **24**, 946–950.
Kurihara, H., Nakano, T., Takasu, N. & Arita, H. (1991). *Biochim. Biophys. Acta*, **1082**, 285–292.
Langlais, J., Chafouleas, J. G., Ingraham, R., Vigneault, N. & Roberts, K. D. (1992). *Biochem. Biophys. Res. Commun.* **182**, 208–214.
Laskowski, R., MacArthur, M., Moss, D. & Thornton, J. (1993). *J. Appl. Cryst.* **26**, 283–290.
Merritt, E. A. & Murphy, M. E. P. (1994). *Acta Cryst.* D**50**, 869–873.
Navaza, J. (1994). *Acta Cryst.* A**50**, 157–163.
Otwinowski, Z. & Minor, W. (1997). *Methods Enzymol.* **276**, 307–326.
Ramachandran, G. N. & Sasisekharan, V. (1968). *Adv. Protein. Chem.* **23**, 283–438.
Roberts, M. F., Deems, R. A. & Dennis, E. A. (1977). *Proc. Natl Acad. Sci. USA*, **74**, 1950–1954.
Rosenthal, M. D., Gordon, M. N., Buescher, E. S., Slusser, J. H., Harris, L. K. & Franson, R. C. (1995). *Biochem. Biophys. Res. Commun.* **208**, 650–656.
Segelke, B. W., Nguyen, D., Chee, R., Xuong, N.-H. & Dennis, E. A. (1998). *J. Mol. Biol.* **279**, 223–232.
Scott, D. L. & Sigler, P. B. (1994). *Adv. Protein Chem.* **45**, 53–88.
Singh, G., Gourinath, S., Sharma, S., Paramasivam, M., Srinivasan, A. & Singh, T. P. (2001). *J. Mol. Biol.* **307**, 1049–1059.

Stahl, U., Ek, B. & Stymme, S. (1998). *Plant Physiol.* **117**, 197–205.
Stahl, U., Lee, M., Sjodahl, S., Archer, D., Cellini, F., Ek, B., Iannacone, R., MacKenzie, D., Semeraro, L., Tramontano, E. & Stymme, S. (1999). *Plant Mol. Biol.* **41**, 481–490.
Sugiyama, M., Ohtani, K., Izuhara, M., Koike, T., Suzuki, K., Imamura, S. & Misaki, H. (2002). *J. Biol. Chem.* **277**, 20051–20058.
Turner, P. J. (1991). *Xmgr* v. 3.01. A plotting tool for workstations using X/Motif. http://plasma-gate.weizmann.ac.il/Xmgr/.
Verheij, H. M., Volwerk, J. J., Jansen, E. H. J. M., Puijk, W. C., Dijkstra, B. W., Drenth, J. & de Haas, G. H. (1980). *Biochemistry*, **19**, 743–750.